Onset of unsteady horizontal convection in rectangle tank at $Pr = 1$

Liang SUN*
School of Earth and Space Sciences, University of Science and Technology of China, Hefei, 230027, China. and LASG, Institute of Atmospheric Physics, Chinese Academy of Sciences, Beijing 100029, China.

Dong-Jun MA, Wei ZHANG, and De-Jun SUN
Dept. of Modern Mechanics, University of Science and Technology of China, Hefei, 230027, China.

arXiv:physics/0702037v3 [physics.flu-dyn] 15 Apr 2008

The horizontal convection within a rectangle tank is numerically simulated. The flow is found to be unsteady at high Rayleigh numbers. There is a Hopf bifurcation of Ra from steady solutions to periodic solutions, and the critical Rayleigh number Ra_c is obtained as $Ra_c = 5.5377 \times 10^8$ for the middle plume forcing at $Pr = 1$, which is much larger than the formerly obtained value. Besides, the unstable perturbations are always generated from the central jet, which implies that the onset of instability is due to velocity shear (shear instability) other than thermally dynamics (thermal instability). Finally, Paparella and Young's first hypotheses about the destabilization of the flow is numerically proved, i.e. the middle plume forcing can lead to a destabilization of the flow.

PACS numbers: 47.20.Bp, 44.25.+f, 92.10.af

Horizontal convection, in which the water is unevenly heated at the horizontal surface, was taken as a model of abyssal ocean circulation. As the abyssal ocean circulation plays an important role in climate change, the horizontal convection has intensively been explored in recent years [1, 2, 3]. It can be set to motion by any small temperature gradient, unlike the Rayleigh-Bénard convection. But similar to Rayleigh-Bénard convection, the horizontal convection may be unsteady at high Rayleigh numbers Ra. There is a critical Rayleigh number Ra_c, and the steady flow is unstable and becomes unsteady when $Ra > Ra_c$. The unsteady flow in horizontal convection was first found by numerical simulation [1], then was observed in the experiment at $Ra > 10^{12}$ [2]. This unsteady flow is proved to be non-turbulent even as $Ra \to \infty$, though the flow field seems to be chaotic [1]. The investigation on the unsteady horizontal convection flow is relatively less, except for [1, 2, 4]. However, they have mainly focused on how the turbulent plume maintains a stable stratified circulation. Yet how the horizontal convection turned to be unsteady remains an elusive problem.

To understand this problem, both Ra_c for the onset of unsteady flow and instability mechanism are of vital. Paparella and Young [1] found $Ra_c \approx 2 \times 10^8$ at $Pr = 1$ in their simulations, which is significantly smaller than others' results [2, 3, 4, 5, 6, 7, 8]. For example, Rossby (1965), Wang and Huang (2005) found the flow is steady and stable for $Ra < 5 \times 10^8$ in their experiments [3, 5]. Yet other numerical simulations [6, 7, 8] have not found unsteady flows for $Ra < 10^9$. Paparella and Young [1] explained the difference of their results from others' as: (i) middle plume forcing in the numerical simulations instead of sidewall plume forcing in the experiments, and (ii) lower aspect ratio ($H/L = 1/4$) in their simulations. Both may lead to destabilization of the flow at lower Rayleigh numbers. However, their hypotheses have not been intensely investigated. According to a recent investigation, the flow is still stable for $Ra < 10^{11}$ even at a much lower aspect ratio ($H/L = 1/10$) [9]. Thus, it maybe the middle plume forcing that leads to destabilization at lower Rayleigh numbers.

Our interest here is to verify their first hypotheses. Is the flow with middle plume forcing less stable than the sidewall plume forcing? How does the instability occur? To investigate these problems, more accurate numerical prediction of Ra_c is need for both forcing cases, for the spatial resolution of simulation was very lower in the past (e.g. 128×32 coarse meshes are used in [1]). Then the flow field under both middle and sidewall plume forcings are compared, which leads to an affirmative answer of the above problem.

Similar to the previous investigations, we consider the horizontal convection flows within the two-dimensional domain, and the Boussinesq approximation is assumed to be valid for these flows. As shown in Fig.1, the horizontal (y) and vertical (z) regimes are $0 \le y \le L$ and $0 \le z \le H$, respectively. Similar to [5], the depth L is taken as reference length scale and $A = H/L = 1/4$ denotes the aspect ratio. Taking account of divergence-free of velocity field in Boussinesq approximation, the Lagrangian streamfunction Ψ and the corresponding vorticity ω are introduced. The velocity $\vec{u} = (v, w)$, where horizontal velocity $v = \frac{\partial \Psi}{\partial z}$ and vertical velocity $w = -\frac{\partial \Psi}{\partial y}$, respectively. The governing equations in vorticity-streamfunction formulation are [1, 7, 10]:

$$\frac{\partial T}{\partial t} + J(\Psi, T) = (\frac{\partial^2 T}{\partial y^2} + \frac{\partial^2 T}{\partial z^2}) \quad (1a)$$

$$\frac{\partial \omega}{\partial t} + J(\Psi, \omega) = - Pr(\nabla^2 \omega + Ra \frac{\partial T}{\partial y}) \quad (1b)$$

$$\nabla^2 \Psi = -\omega \quad (1c)$$

*Electronic address: sunl@ustc.edu.cn;sunl@ustc.edu

TABLE I: Comparison of the benchmark solutions from [11] and [12], $Pr = 0.71$. Ψ_{mid}, $\Psi_{\max}$ are the values in the midpoint and the maximum of streamfunction, respectively. And Nu is average Nusselt number at the heated wall. The resolution is 80×80 meshes for present results.

author	Ra	Ψ_{mid}	$\Psi_{\max}$	Nu
[11]	10^6	16.386	16.811	8.822
[12]	10^6	16.386	16.811	8.825
Present	10^6	16.430	16.863	8.828
[11]	10^7	29.361	30.165	16.523
[12]	10^7	29.356	30.155	16.511
Present	10^7	29.605	30.448	16.535

where $J(\Psi, \phi) = \frac{\partial \Psi}{\partial y}\frac{\partial \phi}{\partial z} - \frac{\partial \phi}{\partial y}\frac{\partial \Psi}{\partial z}$ denotes the nonlinear advection term. There are two important dimensionless parameter in Eq.(1), i.e. Rayleigh number $Ra = \alpha_T \Delta T g L^3/(\kappa\nu)$ and Prandtl number $Pr = \nu/\kappa$, where g, α_T, ΔT, L, κ and ν are gravity acceleration, thermal expansion coefficient, surface temperature difference, length of horizontal domain, thermal diffusivity and kinematic viscosity, respectively. Alternatively, Paparella and Youngs used vertical length H as length scale, so $Ra = 64 Ra_H$, where Ra_H is the vertical Rayleigh number by using vertical length H as unit [1].

More specifically, we consider the horizontal convection in a rectangle tank at $Pr = 1$. The tank has same velocity boundary condition as that in [1], i.e. free slip and no shear stress at the walls. In addition, two different surface forcings are used, which are central symmetric. One is middle plume forcing as $T = [1 + \cos(2\pi y)]/2$ [1], the other is sidewall plume forcing as $T = [1 - \cos(2\pi y)]/2$ [9, 10]. Comparing these with one cell forcing $T = \cos(\pi y/2)$ [6], there are two symmetric cells in the flow field under such forcings (e.g. Fig.1 and Fig.6), when the flow is symmetrically steady and stable. In addition, the middle plume forcing in the left cell is the same with the sidewall plume forcing in the right cell (see Fig.1 behind). Thus in the steady flows, both forcings will lead to the same flow patterns except for a position shift, which is proved by the following investigation.

There are two important quantity describing the circulation, i.e. the non-dimensional streamfunction maximum and the non-dimensional heat flux. The non-dimensional streamfunction maximum $\Psi_{\max} = \Psi^*_{\max}/\nu$, where $\Psi^*_{\max}$ is the maximum of the dimensional streamfunction.

The above Eq.(1) is solved with finite different method in non-uniform grids. Crank-Nicholson scheme and Arakawa scheme [e.g. 13, 14] are applied to discretize the linear and nonlinear terms, respectively. Comparing to the other schemes, Arakawa scheme is more accurate but more expensive, and it has also been applied to horizontal convection flows at high Rayleigh number [8, 9]. Table I shows the validation of the scheme with nature convection problem. A fine spatial resolution mesh of 512×128 is used to eliminate numerical instability.

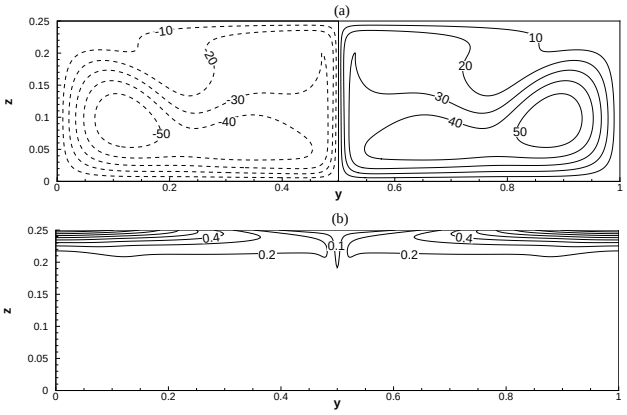

FIG. 1: The flow stream function (a) and temperature field (b) of $Ra = 5 \times 10^8$. It is steady and stable and symmetric with middle plume forcing, solid and dashed curves for positive and negative values, respectively.

First, the middle plume forcing is considered, which is steady and stable for $Ra < 5.5 \times 10^8$. Fig.1 shows the flow field (a) and temperature field (b) of $Ra = 5 \times 10^8$ with $\Psi_{\max} = 59.83$, in which the flow is symmetric, steady and stable. In this case, the center line symmetrically separates the flow field into two parts, like a free slip wall. There is a vigorous downward jet in the center of tank corresponding to the middle plume forcing (Fig.1a), where the vertical velocity field has a minimum of $w = -2513$ (Fig.2b). The center jet leads to the clockwise and anticlockwise plume cells in the left and right part of tank, respectively. In the left circulation cell, the flow sinks quickly along the center line and upwells clockwise along the left side wall with relatively slower speed, which can be also seen from the vertical velocity of the flow (Fig.2). Besides, there are two horizontal jets respectively near top and bottom walls in the left circulation cell (Fig.2a). Totally, there are 2 horizontal jets near wall and a vertical jet at the center in each cell. Contract to the flow field, the temperature field is very simple. An obvious boundary layer exists near the surface in temperature field, which leads to a 1/5-power law of Ra for heat flux [e.g. 5, 7, 10]. And below the temperature boundary layer, the temperature is almost homogeneous due to the convection. Thus there is a very strong stratification near the surface ($\partial T/\partial z \sim Ra^{1/5}$) but a very weak stratification in other region ($\partial T/\partial z \sim 0$). As the above case is stable, so the critical Rayleigh number must be larger than 5×10^8, which is significantly larger than the value obtained before [1].

To find the critical Rayleigh number Ra_c, the growth rate of perturbation $\phi(t)$ is calculated numerically. And $\phi(t)$ is assumed to satisfy $\phi(t) = e^{\sigma t}\phi(0)$, where $\sigma = \sigma_r + i\sigma_i$ is the complex growth rate of disturbance. It is found that the onset of unsteady flow is at $Ra_c = 5.5377 \times 10^8$, as shown in Fig.3. For $Ra = 5.53 \times 10^8$, the flow is stable and the growth rate is approximately $\sigma_r = -0.12$. But the flow is unstable and the growth rate is approximately

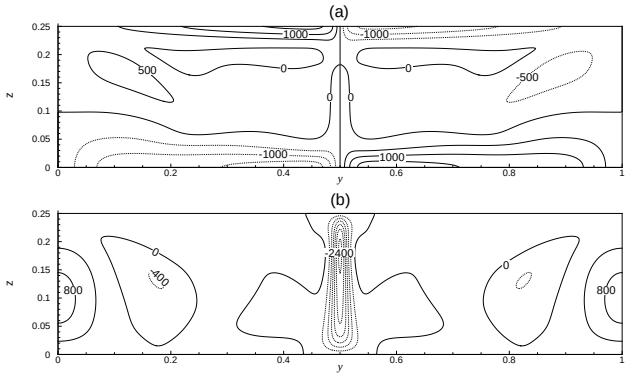

FIG. 2: The horizontal (a) and vertical (b) velocity fields of $Ra = 5 \times 10^8$. It is steady and stable and symmetric with middle plume forcing, solid and dashed curves for positive and negative values, respectively.

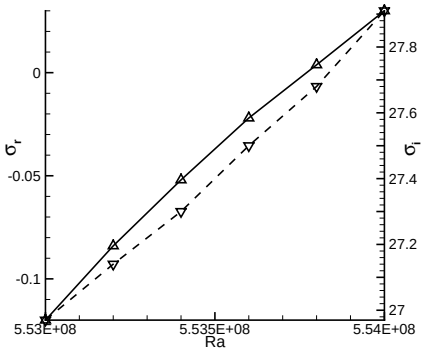

FIG. 3: Growth rate σ_r (solid) and σ_i (dashed) vs. Ra, respectively.

$\sigma_r = 0.03$ for $Ra = 5.54 \times 10^8$. Thus the critical Rayleigh number Ra_c is obtained $5.53 \times 10^8 < Ra_c < 5.54 \times 10^8$. The accurate value of $Ra_c = 5.377 \times 10^8$ is obtained by interpolating from the above result. Moreover, the onset of unsteady flow is found to occur via Hopf bifurcation. As Fig.3 shows, the image part of growth rate is nonzero and the eigenmode of perturbation is periodic. This Hopf bifurcation of the horizontal convection has not been reported yet, and previous investigations dealt only with chaotic flows.

Meanwhile, the evolution of the perturbation vorticity fields during the first half period at $t = 0$ (a), $t = T/8$ (b), $t = T/4$ (c) and $t = 3T/8$ of $Ra = 5.54 \times 10^8$ are depicted in Fig.4, respectively. The perturbation vorticity fields are symmetric about centerline, which implies that the horizontal velocity is nonzero at centerline. It can be seen that the perturbation tripole A (the shadowed ellipse in Fig.4a) is generated from central downward jet, then propagates and amplifies along the central jet downward to the bottom wall (Fig.4b,c,d). When tripole A approaching to the bottom, it becomes weaker and weaker and breaks into two parts: the left and the right near the

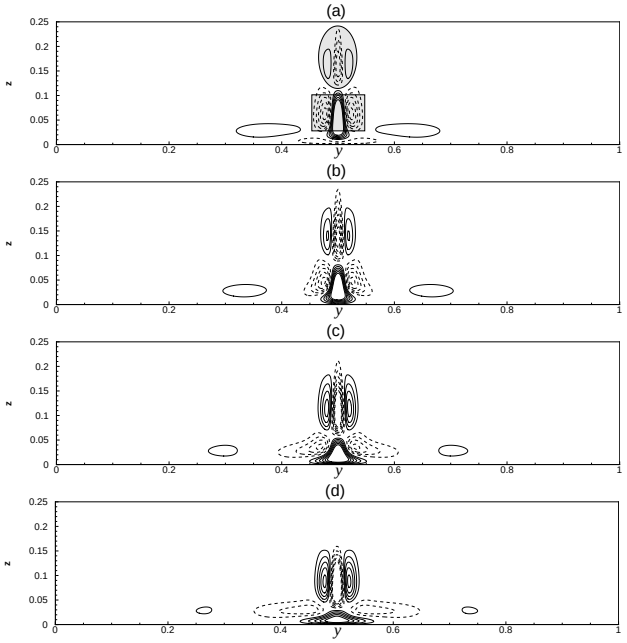

FIG. 4: The perturbational vorticity fields at $t = 0$ (a), $t = T/8$ (b), $t = T/4$ (c) and $t = 3T/8$ of $Ra = 5.54 \times 10^8$, solid and dashed curves for positive and negative values, respectively.

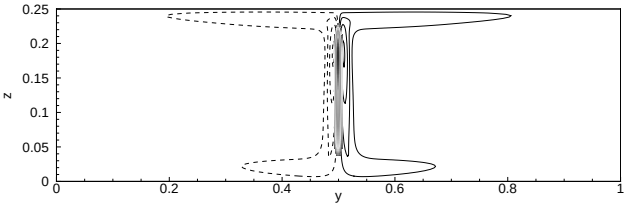

FIG. 5: The vorticity of $Ra = 5.54 \times 10^8$ with vertical velocity w (shadowed as $w > 1800$), solid and dashed curves for positive and negative values, respectively.

bottom, which can be seen from the evolution of tripole B (the shadowed rectangle in Fig.4a). And the mean flow advects the broken vortexs horizontally along the bottom wall (Fig.4b,c,d). Then in the second half period, a reverse tripole will generate the same place of vortexes A at $t = T/2$, and the same story repeats for it, which is omitted here. In short, the perturbations generate and amplify in the central vertical jet, but are propagated and weakened along the horizontal wall.

Further investigation shows that the instability of flow occurs due to shear. First, as we noting, the instabilities always occur in the center and propagate along the mean flow. Second, this trigger place locates in the area where there is a vigorous jet with strong shear (see e.g. Fig.2b and Fig.5) (Fig.5). As the stratification is very weak here (see e.g. Fig.1b), the flow in this region is dominated by momentum dynamics other than thermal dynamics. All these imply that the onset of instability leading to un-

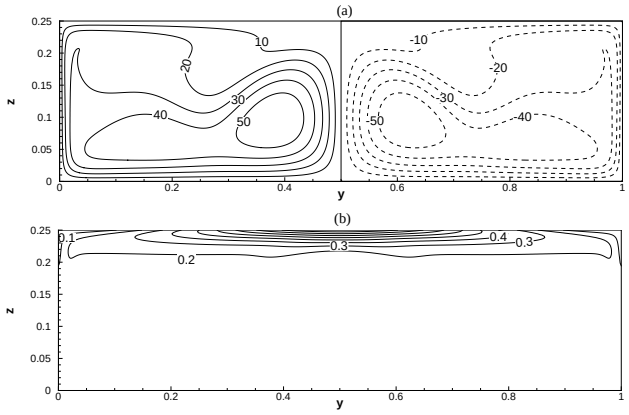

FIG. 6: The flow field (a) and temperature field (b) of $Ra = 5 \times 10^8$, which are steady and stable and symmetric with sidewall plume forcing.

steady flow is due to shear instability at larger Rayleigh numbers, which is much different from Rayleigh-Bénard instability. However, shear is not the sufficient condition for instability. For example, the instability near the top surface is suppressed due to strong stratification (Fig.1b), though both the velocity (Fig.2a) and the shear (Fig.5) near top surface are still very large. In words, the onset of instability is due to velocity shear (shear instability) other than thermally dynamics (thermal instability).

Now, the sidewall plume forcing is considered. Fig.6 shows the flow field and temperature field of $Ra = 5\times10^8$, in which the flow is symmetric, steady and stable like that under middle plume forcing. There are two vigorous downward jets near the walls corresponding to the sidewall plume forcing (Fig.6a). As mentioned above, the sidewall plume forcing will lead to exactly the same flow pattern as the middle plume forcing does except for a position shift, which can be seen from Fig.1 and Fig.6. As the flow is stable, the center line like a free slip wall symmetrically separates the two cells. The left cell in Fig.1 is exactly the same with the right cell in Fig.6. However, the flow is much more stable with the sidewall plume forcing. And the critical Rayleigh number is found $Ra_c \approx 1.85\times10^{10}$ (with 768×192 meshes) in this case. As mentioned above, the flow is much more stable with the sidewall plume forcing than that with the middle plume forcing, though both forcings lead to the same flow patterns. This is very interesting, and can be understood from the mechanism of instability.

It's found that the rigid wall suppresses the perturbation, which leads a more stable flow with the sidewall plume forcing than that with the middle plume forcing. As the loss of stability is due to strong velocity shear in the center in horizontal convection, the smaller the shear is, the more stable the flow is. In the case of middle plume forcing, the perturbation with nonzero horizontal velocity occurs at the most vigorous downward jet. And the perturbed flows cross the center line and propagate downstream. However, in the case of sidewall plume forcing, these crossing flows are suppressed by rigid walls. So that the critical Rayleigh number is much larger in this case. Paparella and Young (2002) hypothesized that middle plume forcing may lead to a destabilization of the flow. Here this hypotheses is proved both physically and numerically.

In conclusion, the onset of unsteady flow is found to occur via a Hopf bifurcation in the regime of $Ra > Ra_c = 5.5377 \times 10^8$ for the middle plume forcing at $Pr = 1$, which is much larger than the previously obtained value. Besides, the onset of unsteady flow is due to shear instability of central downward jet. Finally, the first hypotheses of Paparella and Young (2002) for instability is numerically approved, i.e. the middle plume forcing can lead to a destabilization of the flow at relatively lower Rayleigh numbers.

This work is supported by the National Basic Research Program of China (No. 2007CB816004), the National Foundation of Natural Science (No. 40705027, No. 10602056 and No. 10772172), the National Science Foundation for Post-doctoral Scientists of China (No. 20070410213), and the Presidential Foundation of the Chinese Academy of Sciences, China.

[1] F. Paparella and W. R. Young, J. Fluid Mech. **466**, 205 (2002).
[2] J. C. Mullarney, R. W. Griffiths, and G. O. Hughes, J. Fluid Mech. **516**, 181 (2004).
[3] W. Wang and R. X. Huang, J. Fluid Mech. **540**, 49 (2005).
[4] G. O. Hughes, R. W. Griffiths, J. C. Mullarney, and W. H. Peterson, J. Fluid Mech. **581**, 251 (2007).
[5] H. T. Rossby, Deep-Sea Research **12**, 9 (1965).
[6] H. T. Rossby, Tellus **50A**, 242 (1998).
[7] J. H. Siggers, R. R. Kerswell, and N. J. Balmforth, J. Fluid Mech. **517**, 55 (2004).
[8] L. Sun, Y. F. Sun, D. J. Sun, and X. Y. Yin, Journal of Hydrodynamics A **21**, 252 (2006).
[9] L. Sun, Y. F. Sun, D. J. Ma, and D. J. Sun, Acta Physica Sinica **56**, 6503 (2007).
[10] C. Quon and M. Ghil, J. Fluid Mech. **245**, 449 (1992).
[11] P. Le Quéré, Computers and Fluids **20**, 29 (1991).
[12] Z. Tian and Y. Ge, Int. J. Numer. Meth. Fluids **41**, 495 (2003).
[13] A. Arakawa, J. Comput. Phys. **1**, 119 (1966).
[14] P. Orlandi, *Fluid flow phenomena* (Kluwer Academic publishers, Dordrecht, The Netherlands, 2000).